



HAL
open science

Temporal and spatial trends in aerosols near the English Channel – An air quality success story?

Mingxi Yang, Joelle C.E. Buxmann, Hervé Delbarre, Marc Fourmentin, Tim Smyth

► **To cite this version:**

Mingxi Yang, Joelle C.E. Buxmann, Hervé Delbarre, Marc Fourmentin, Tim Smyth. Temporal and spatial trends in aerosols near the English Channel – An air quality success story?. *Atmospheric environment: X*, 2020, 6, pp.100074. 10.1016/j.aeaoa.2020.100074 . hal-04290689

HAL Id: hal-04290689

<https://ulco.hal.science/hal-04290689>

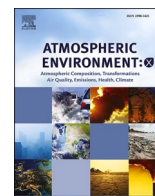
Submitted on 19 Feb 2024

HAL is a multi-disciplinary open access archive for the deposit and dissemination of scientific research documents, whether they are published or not. The documents may come from teaching and research institutions in France or abroad, or from public or private research centers.

L'archive ouverte pluridisciplinaire **HAL**, est destinée au dépôt et à la diffusion de documents scientifiques de niveau recherche, publiés ou non, émanant des établissements d'enseignement et de recherche français ou étrangers, des laboratoires publics ou privés.

Contents lists available at [ScienceDirect](https://www.sciencedirect.com)

Atmospheric Environment: X

journal homepage: <http://www.journals.elsevier.com/atmospheric-environment-x>

Temporal and spatial trends in aerosols near the English Channel – An air quality success story?

Mingxi Yang^{a,*}, Joelle C.E. Buxmann^b, Hervé Delbarre^c, Marc Fourmentin^c, Tim J. Smyth^a^a Plymouth Marine Laboratory, Plymouth, PL1 3DH, UK^b UK Met Office, Exeter, UK^c Laboratoire de Physico-Chimie de l'Atmosphère, Université du Littoral-Côte d'Opale, Dunkerque, France

ABSTRACT

We present a detailed analysis of long-term aerosol measurements from four sun photometer sites (from west to east: Plymouth, Chilbolton, Dunkirk, Oostende) and four Department for Environment, Food & Rural Affairs surface sites (from west to east: Plymouth, Southampton, Portsmouth, Eastbourne) near the English Channel. From the early 2000s to about 2016, annual mean Aerosol Optical Depth (AOD) from all sun photometer sites decreased by an overall average of 23% decade⁻¹ (range of 15–28% decade⁻¹). From 2010 to 2017, annual mean concentration of particulate matter with aerodynamic diameter less than 2.5 μm (PM_{2.5}) from all the surface sites decreased by an overall average of 44% decade⁻¹ (range of 7–64% decade⁻¹). Seasonally, the highest aerosol loading is generally found around the springtime, and this maximum has been decreasing much faster over recent years than during the other seasons. This is driven by the interaction between the seasonal weather patterns (e.g. reduced westerly flow and drier weather in the spring) and the main emission sources being predominantly from the European Continent. We find clear spatial gradients in the aerosol loading as well as aerosol composition. From west to east along the English Channel, PM_{2.5} concentration increases with a mean gradient of about 0.007 μg m⁻³ km⁻¹. At the westernmost site Plymouth, sea spray is estimated on average to account for 16% of the AOD and 13% of the particulate matter with aerodynamic diameter less than 10 μm (PM₁₀). The importance of sea spray is reduced by at least a factor of two at the more eastern sites. The long-term decrease in aerosol loading along the English Channel appears to be more strongly driven by the reduced anthropogenic emissions, rather than by changes in the large-scale circulation such as the North Atlantic Oscillation. Clean ups in road vehicles and ship emissions, however, do not appear to be strong drivers for the long-term trends in aerosol loading at these coastal sites.

1. Introduction

Aerosols affect atmospheric chemistry, visibility, and the Earth's radiative balance. Because of their impact on human health, aerosols are one of the principal indicators of air quality (e.g. Pope et al., 2009; Lelieveld et al., 2017). At the confluence of several interfaces, coastal environments (especially coastal cities) are exposed to multiple sources of aerosols or their precursors depending on wind direction and air mass history. These include terrestrial pollution, ship emissions, and sea spray (e.g. Zielinski, 2004). As a result of this complexity, there remain significant uncertainties in aerosol budgets over land close (<60 km) to the coast, where a large fraction of the population resides (e.g. over 90% for the United Kingdom).

Thanks to a series of regulations (e.g. the Clean Air Act), terrestrial anthropogenic emissions of aerosol precursors, in particular sulfur and nitrogen oxides, have significantly reduced in Western Europe over the last two decades. Several studies have reported reductions in the aerosol loading over Europe since the 2000s (de Meij et al., 2012; Mao et al., 2014; Yoon et al., 2016; Zhao et al., 2017; Ningombam et al., 2019),

coinciding with the aforementioned emission reductions. Despite this welcoming trend, exceedances in aerosol concentrations over air quality regulations over Europe still occur (<https://www.eea.europa.eu/data-and-maps/indicators/main-anthropogenic-air-pollutant-emissions/assessment-4>). There is also considerable uncertainty about which sectors are responsible for the trend in the aerosol loading and in the present day aerosol composition (e.g. Curci et al., 2015; Kristiansen et al., 2016).

Ship exhaust emissions have the potential to significantly affect the atmospheric chemistry and air quality in coastal environments. For example, ships generally burn low quality, high-sulfur fuel, and so emitting about 10 Tg (teragram) of sulfur dioxide (SO₂) into the atmosphere globally every year (Johansson et al., 2017). Most of that SO₂ is subsequently converted to submicron sulfate aerosols. Within 'Sulfur Emission Control Areas' (SECAs), including the English Channel, the International Maritime Organisation (IMO) has implemented stage-wise reductions in the maximum ship sulfur emission. Reported as % of sulfur emitted per mass of fuel, the maximum allowed fuel sulfur content has reduced from 1.5% (pre-July 2010), to 1% (post-July 2010), to 0.1%

* Corresponding author.

E-mail address: miya@pml.ac.uk (M. Yang).<https://doi.org/10.1016/j.aeoa.2020.100074>

Received 27 November 2019; Received in revised form 18 March 2020; Accepted 27 March 2020

Available online 8 April 2020

2590-1621/Crown Copyright © 2020 Published by Elsevier Ltd. This is an open access article under the CC BY license (<http://creativecommons.org/licenses/by/4.0/>).

(post-January 2015). A ~ 3 -fold reduction in the atmospheric SO_2 burden has been observed from 2014 to 2015 in air masses passing over the Penlee Point Atmospheric Observatory on the southwest coast of the UK in response to the more recent sulfur regulation (Yang et al., 2016). The impact of these regulations on the coastal aerosol budgets remains under-explored.

When waves break, whitecaps (bubbles visible on the sea surface) are formed, generating sea spray aerosols (Lewis and Schwartz, 2004). The whitecap fraction is generally parameterized by a cubic relationship with wind speed (e.g. Monahan, 1986). Whilst most of the sea spray mass has a mode diameter of a few microns, sea spray aerosols ranging from about 20 nm to a millimeter are produced (Wang et al., 2017). The largest sea spray aerosols settle out of the atmosphere very quickly, while smaller aerosols can be advected over long distances. In coastal environments, waves shoal upon entering shallower water and break more readily. Observations generally show an approximately one order of magnitude higher sea spray production fluxes near the coast than over the open ocean at similar wind speeds (de Leeuw et al., 2011; van Eijk et al., 2011; Andreas, 2016). Mulcahy et al. (2008) found that AOD at Mace Head, Ireland during periods of clean marine air exhibited a strong wind speed dependence and attributed it to sea spray. Yang et al. (2019) showed that sea spray production at the coast depend on both wind speed and significant wave height.

Here we analyze aerosol observations from four sun photometer sites (Plymouth, Chilbolton, Dunkirk, and Oostende; from the early 2000s to ~ 2016) and four surface air quality stations (Plymouth, Southampton, Portsmouth, and Eastbourne; from 2010 to 2017) near the English Channel (Fig. 1). We choose to study these sites near the shore because of the aforementioned importance of coastal air quality, and also because of the relative scarcity of coastal aerosol studies. The long-term variability, seasonal variability, and spatial variability in aerosols are presented in the Results section. For the spatial variability analysis, we derive an AOD:PM_{2.5} relationship derived from co-located remote and surface observations in Plymouth, test this relationship with the surface PM_{2.5} measurements at Dunkirk, and then apply it to other sun photometer sites. In the Discussion section, we explore the different possible drivers to the observed variability in aerosols, including

anthropogenic emissions, sea spray, and changes in general circulation.

2. Theory and methods

Aerosol optical depth (AOD) is a measure of aerosol light extinction integrated over the entire atmospheric column. Many studies on recent trends in aerosols utilize AOD derived from visible channel satellite data (e.g. MODIS, Moderate resolution Imaging Spectroradiometer) (Mehta, 2016; Zhao et al., 2017, Glantz et al., 2019), a measurement that is very sensitive to sensor drift and corrections (Angal et al., 2013; Sun et al., 2015). Ground-based sun photometer measurements (e.g. from the aerosol robotic network, AERONET; or Sky Radiometer Network, SKYNET), with an accuracy and precision better than 0.01 AOD at 500 nm (Holben et al., 1998; Eck et al., 1999), provide an alternative way to examine the temporal and spatial trend in the aerosols.

Most (ca. 90%) of the light extinction caused by aerosol is due to scattering, and small aerosols scatter short wavelength (λ) light more effectively than long wavelength light (Seinfeld and Pandis, 2006). The Ångström exponent describes the wavelength-dependence in aerosol extinction, and here is computed from 400 (or 440) nm to 870 nm as a linear regression of $\log_e(\text{AOD})$ vs. $\log_e(\lambda)$. Large (i.e. supermicron) aerosols, such as sea spray, are generally associated with a lower Ångström exponent (e.g. Estellés et al., 2012b), while small (i.e. submicron) aerosols from pollution generally have a higher Ångström exponent.

Here we use Version 2 Level 2.0 data (cloud-screened and quality-controlled) from three CIMEL sun photometers in Chilbolton, Dunkirk, and Oostende. Daily averaged data were downloaded from AERONET (<https://aeronet.gsfc.nasa.gov/>). These CIMEL sun photometers operate at (340, 380), 440, 500, 675, 870, and 1020 nm. Sun photometer data from Plymouth are from a PREDE POM instrument, which is a part of SKYNET. This instrument (on top of the Plymouth Marine Laboratory building, less than 1 km from the Plymouth surface site as described below) includes channels at 400, 500, 675, 870 and 1020 nm. The POM data are cloud-screened using a method similar to Smirnov et al. (2000) using AOD at 1020 nm. Previous intercomparisons of a CIMEL and a POM Sun photometer in Plymouth yielded very good agreement of AOD within the uncertainty of 0.01–0.02 in the spectral range 400–1020 nm. For the Ångström exponent the difference is less than 0.02 (Estellés et al., 2012a). In order to compare sun photometer data from different sites and facilitate comparisons against MODIS, we interpolate AOD to a common wavelength of 550 nm using the measured Ångström exponent. Gaps in the time series were generally due to instrument faults.

Ground-level particulate matter (PM) is measured at the Department for Environment, Food & Rural Affairs (DEFRA) Automatic Urban and Rural Network (AURN) stations in Plymouth, Southampton, Portsmouth and Eastbourne. These four stations are all classified by DEFRA as ‘urban background’ sites. The PM concentrations are quantified using a Thermo tapered element oscillating microbalance (TEOM 1400AB) and Filter Dynamics Measurement System (FDMS 8500). In addition to providing total PM_{2.5} and PM₁₀ (particulate matter less than 2.5 and 10 μm , respectively), the aerosols are further separated into (semi) volatile and non-volatile components. Daily averaged data are downloaded from the DEFRA website (<https://uk-air.defra.gov.uk/data/>).

Ground-level PM is measured in Dunkirk by the French air quality network ATMO ‘Hauts-de-France’ in northern France). Two stations, using TEOM-FDMS, monitor PM_{2.5} concentration at Malo-Les-Bains on the coast (DK4) and the eastern part of the industrial area, and at Cappelle-La-Grande at about 7 km from the coast (DKH) and south of industrial area. DK4 and DKH are respectively classified as urban and periurban stations. Daily and hourly averages data are available from the ATMO Hauts-de-France web site (<https://www.atmo-hdf.fr/>).

Direct sun photometer measurements can only be made when there are no clouds in front of the sun, resulting in more data in the drier spring/summer. Coupled to the much shorter daylight in winter (as little as 8 h) than in summer (as much as 16 h), there are generally far fewer valid sun photometer measurements in the winter. As a result, yearly

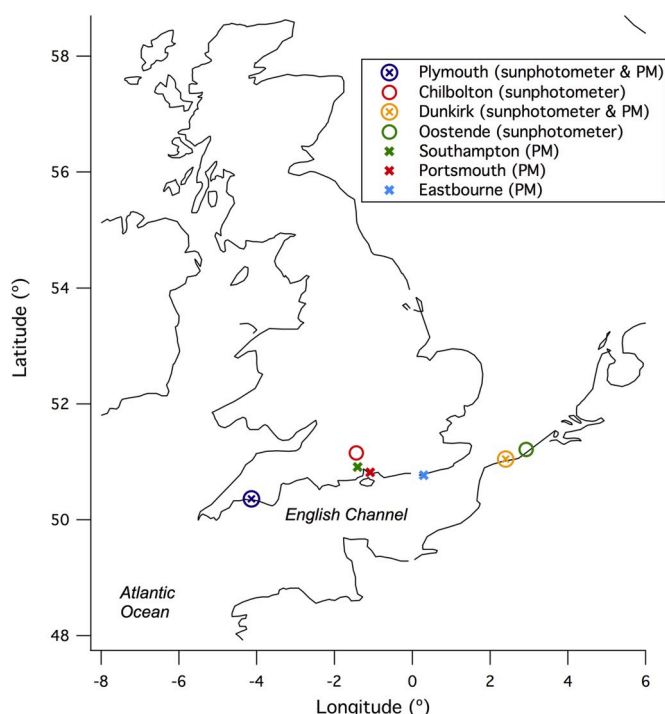


Fig. 1. Sites with sun photometer (circle) and PM (cross) data.

means in AOD computed directly from the high frequency observations tends to result in a ‘summer bias.’ To ensure more equal representation of all seasons in our trend analysis, we first average the daily observations to monthly-bins, and then average the monthly-bins to yearly bins (taking advantage of the fact that even in winter, there are generally still at least a few days of valid measurements in a month).

PM measurements are continuous and do not suffer from such a seasonal bias. For the sake of consistency we analyze the long-term PM trends the same way. In contrast to the columnar AOD, PM is more sensitive to changes in the planetary boundary layer height and vertical

mixing (e.g. sea-breeze effect and diurnal variability). This ground-level measurement is a more directly relevant parameter for public health as it better reflects the environment that people experience.

3. Results

Aerosol loading along the English Channel is subject to the strong contrast between the marine airmasses coming off the North Atlantic from the southwest quadrant (ca. 50% of the time), and the European continental airmasses from the east/southeast (ca. 20% of the time). The

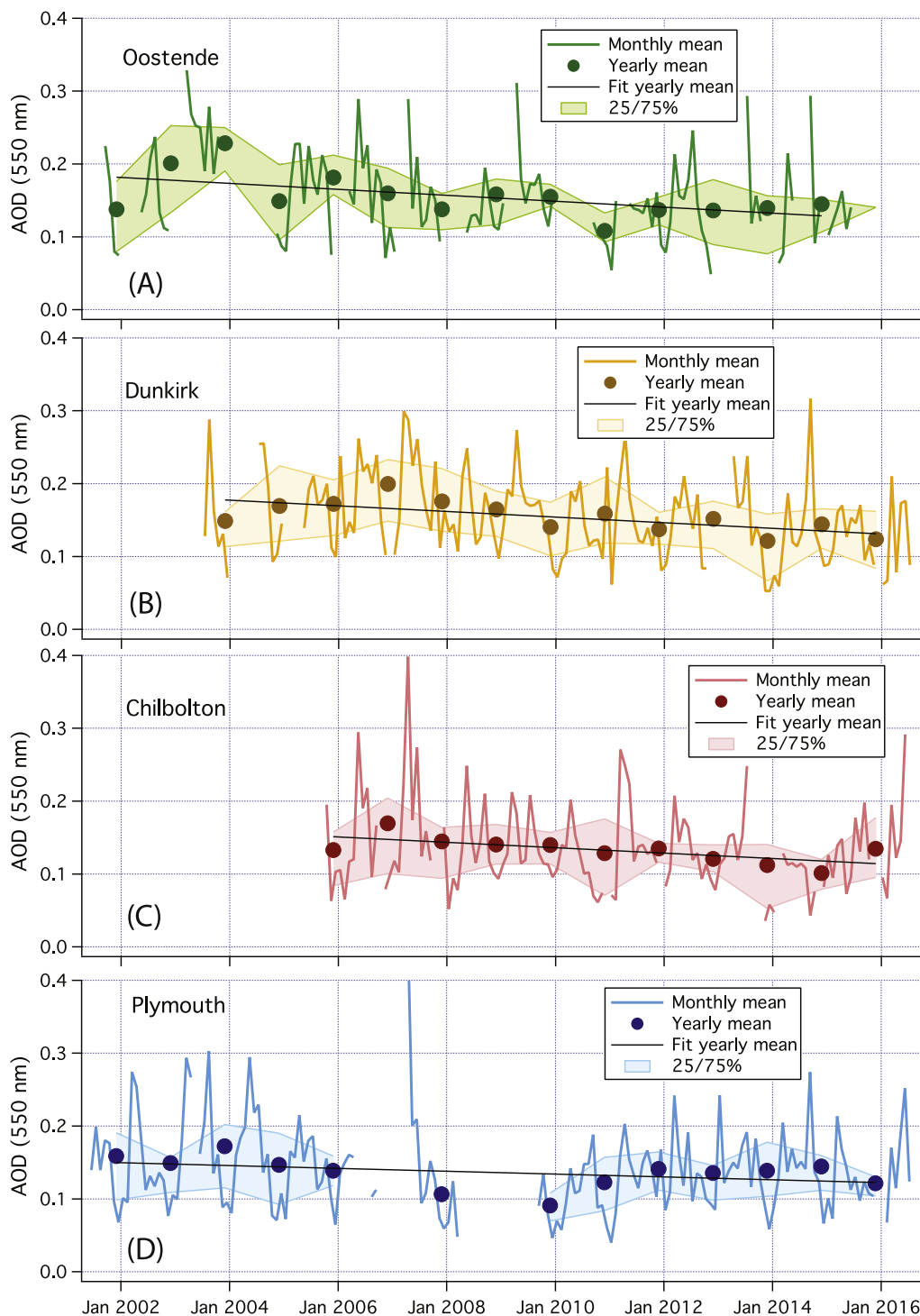


Fig. 2. Time series of AOD at Oostende (A), Dunkirk (B), Chilbolton (C), and Plymouth (D): monthly mean, yearly mean, linear fit to yearly mean, and 25 and 75 percentiles of monthly data.

prevailing southwesterly winds are well aligned with the orientation of the English Channel, facilitating longer-range transport of marine aerosols and accumulation of pollutants along the way. Seasonally, high wind speeds from the southwest and heavy precipitation occur the most frequently in the winter half of the year. The spring/early summer is characterized by relatively more prevalent winds from the east as well as dryer conditions.

The long-term trends, seasonal variability, and spatial variability of aerosols along the English Channel are presented in Sections 3.1, 3.2, and 3.4, respectively. In Section 3.3, we use co-located measurements of AOD and PM in Plymouth to derive an empirical relationship between AOD and PM2.5, which is used in the spatial variability analysis.

3.1. Long-term trends in aerosol loading

Fig. 2 shows time series of AOD550 (monthly mean, yearly mean, fit to yearly mean, and 25th and 75th percentiles) from the four sun photometer sites. AOD has decreased since the early/mid 2000s at Chilbolton, Dunkirk, and Oostende at a similar rate of just under 0.04 decade⁻¹ (which amounts to ~23% of the mean AOD during this period). As summarized in Table 1, this reduction is statistically significant at 95% confidence level. These rates of decrease are consistent with previous findings based on satellite (e.g. Mao et al., 2014; Zhao et al., 2017) and ground based observations (e.g. Yoon et al., 2016; Ningombam et al., 2019). The decrease in Plymouth (0.02 decade⁻¹, or 15%) is less obvious, probably in part to data gaps in the late 2000s. The interannual variability in AOD550, here roughly estimated as one standard deviation of the linearly de-trended annual mean, is 0.025, 0.016, 0.013, and 0.019 for Oostende, Dunkirk, Chilbolton, and Plymouth, respectively. These values amount to 10–16% of mean AOD550 at these sites, and roughly half of the magnitude of the decadal change.

We can compare the proportional decrease in AOD at 400, 550, and 1020 nm. At most sites, the proportional decrease at 1020 nm is as rapid as at the shorter wavelengths. The Ångström exponent does not demonstrate any significant long-term trends at any of the sites analyzed here (Table 1). These results suggest that the modal aerosol size for the small aerosols has not changed substantially despite the overall decrease in burden. Changes in aerosol size and composition are discussed further in Section 4.

Fig. 3 shows the time series in PM2.5 and PM10 (monthly mean, yearly mean, fit to yearly mean) at Eastbourne, Portsmouth, Southampton, and Plymouth from late 2010 to mid-2017. The correlation in aerosols at different sites is significant, and is largely driven by their seasonality (see Section 3.2). For example, monthly mean PM2.5 in Plymouth and Eastbourne (the two sites furthest apart) have an R² value of 0.51. The high degree of correlation at these different coastal sites reflects the connected airflow along the English Channel and the fairly long lifetime of these small aerosols.

Portsmouth, Southampton, and Eastbourne show large decreases ranging from 6.5 to 8.5 µg m⁻³ decade⁻¹ in PM2.5, which amount to around 50% of their respective means during this period (Table 2). Intriguingly, mean PM10 level at these surface sites have only decreased slightly (not significant at 95% level). Plymouth stands out as an exception. AOD and PM2.5 have not significantly decreased in Plymouth, but PM10 has (the latter by about 37% decade⁻¹).

Table 1
Summary from sun photometer sites.

Site	Duration	Days of data	<AOD>	<Ang>	dAOD/dt	dAng/dt	d(AOD _{MAMJ})/dt	d(AOD _{NDJF})/dt
Oostende	2001–2015	1552	0.154	1.119	-0.037 (0.015)	0.014 (0.085)	-0.079 (0.016)	-0.002 (0.015)
Dunkirk	2003–2016	1780	0.164	1.087	-0.039 (0.012)	-0.016 (0.115)	-0.072 (0.025)	-0.040 (0.016)
Chilbolton	2005–2016	1346	0.134	1.099	-0.037 (0.013)	0.117 (0.053)	-0.082 (0.027)	-0.019 (0.019)
Plymouth	2001–2016	1708	0.136	0.797	-0.020 (0.012)	-0.017 (0.053)	-0.042 (0.016)	-0.007 (0.013)

Notes: <> signifies mean; trends per decade; AOD at 550 nm; Ångström exponent (Ang) computed from 400 to 870 nm; standard deviation in parentheses; significant (95% confidence level) trends boldfaced; MAMJ: March to June, NDJF: November to February.

The interannual variability in PM2.5 (1 standard deviation of the de-trended annual mean) is 2.0, 1.0, 0.9, and 1.0 µg m⁻³ for Eastbourne, Portsmouth, Southampton, and Plymouth, respectively. These values amount to 7–15% of the mean PM2.5 at these sites, proportionally comparable to the interannual variability in AOD. In comparison, the interannual variability in PM10 (normalized by their means) is slightly lower at 5–10% at these sites.

3.2. Seasonal variability in the aerosols

The seasonality in aerosols is driven by different sources and sinks as well as atmospheric transport. AOD at these coastal sites consistently show springtime maxima and wintertime minima. The seasonally averaged AOD (550 nm) at Oostende, Dunkirk, and Chilbolton are fairly similar, ranging from 0.1 or less in the winter to over 0.2 in the spring (Fig. 4A). As shown in the previous section, AOD at all sites have been declining over the last decade. The Chilbolton dataset starts in late 2005, a few years later than the other datasets. Thus the mean AOD from Chilbolton in Fig. 4A could be biased low slightly relative to the other sun photometer sites.

The Ångström exponents at all sites follow a qualitatively similar pattern, with the highest values in the summer and the lowest values in the winter (Fig. 4A). The Ångström exponent at Plymouth is on average ~0.3 lower than at other sites, with a difference that is greater in the winter than in the summer. This is because amongst these sites, the westernmost (Plymouth) has the highest sea spray contribution to AOD (see Section 4.2). The mean seasonality in Plymouth shown here is consistent with an earlier analysis of the Plymouth data by Estellés et al. (2012b).

The seasonal variability in PM demonstrates similarities as well as differences to those of AOD (Fig. 4, bottom panel). As with AOD, PM2.5 and PM10 also peak near the spring. The mean PM2.5:PM10 ratio ranges from ~0.6 in Plymouth to ~0.7 at the other sites (see supplement Fig. S1). This ratio peaks in the spring (over 0.7 in Plymouth and 0.9 in Portsmouth), implying that the greater aerosol loading around the spring is mostly due to small aerosols (more likely to be of anthropogenic origin; see Section 4.1). That the lowest PM2.5:PM10 ratio is found in Plymouth can again be attributed to the greater importance of sea spray at this westernmost site (see Section 4.2).

Unlike AOD, both PM2.5 and PM10 display summertime minima (Fig. 4, bottom panel), probably in part due to the deepening of the planetary boundary layer (PBL). At this latitude and over the sea, the mean PBL height is on the order of 60% greater in the summer due to increased convection than in winter (Chan and Wood, 2013). This causes more dilution of surface emissions and so reduces PM at ground level, consistent with previous analyses of aerosol profiles (e.g. Zhao et al., 2018). AOD, being an atmospheric column measurement, is insensitive to such boundary layer height changes. The AOD values at these coastal sites are about 20% lower in the summer than in the spring, while PM2.5 concentrations at nearby coastal sites are nearly half as much in the summer compared to the spring. It appears that the seasonality in PBL can approximately account for the apparently different seasonality in AOD and in PM2.5.

To explore changes in the seasonality of aerosols, we separate the AOD data to the spring/early summer (March to June) and winter

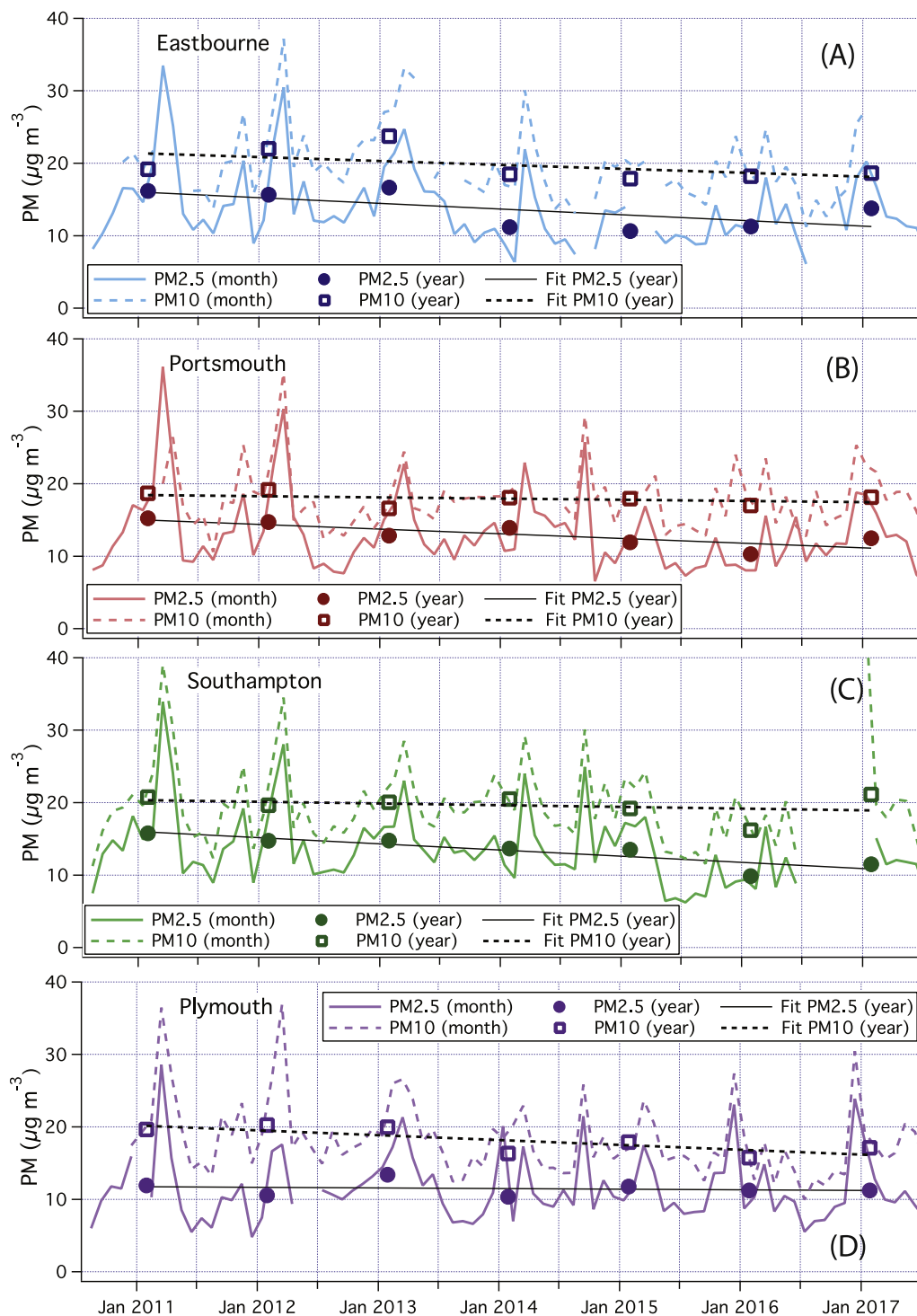


Fig. 3. Time series of PM2.5 and PM10 at Eastbourne (A), Portsmouth (B), Southampton (C), and Plymouth (D): monthly mean, yearly mean, and fits to yearly mean.

Table 2
Summary from DEFRA surface sites.

Site	Duration	Days of data	<PM2.5>	<PM10>	d(PM2.5)/dt	d(PM10)/dt	d(PM2.5 _{MA})/dt	d(PM2.5 _{NDJF})/dt
Eastbourne	2010–2017	2196	13.62	19.73	-7.86 (4.07)	-5.37 (3.97)	-27.01 (5.77)	-5.76 (6.31)
Portsmouth	2010–2017	2343	13.05	17.94	-6.46 (2.07)	-1.64 (1.69)	-26.95 (4.07)	-6.81 (5.58)
Southampton	2010–2017	2123	13.39	19.63	-8.52 (1.93)	-2.36 (3.25)	-25.00 (4.60)	-5.95 (5.20)
Plymouth	2010–2017	2121	11.48	18.13	-0.84 (2.07)	-6.65 (2.34)	-15.63 (5.20)	5.27 (3.50)

Notes: <> signifies mean; PM in $\mu\text{g m}^{-3}$; trends per decade; standard deviation in parentheses; significant (95% confidence level) trends boldfaced; MA: March to April, NDJF: November to February.

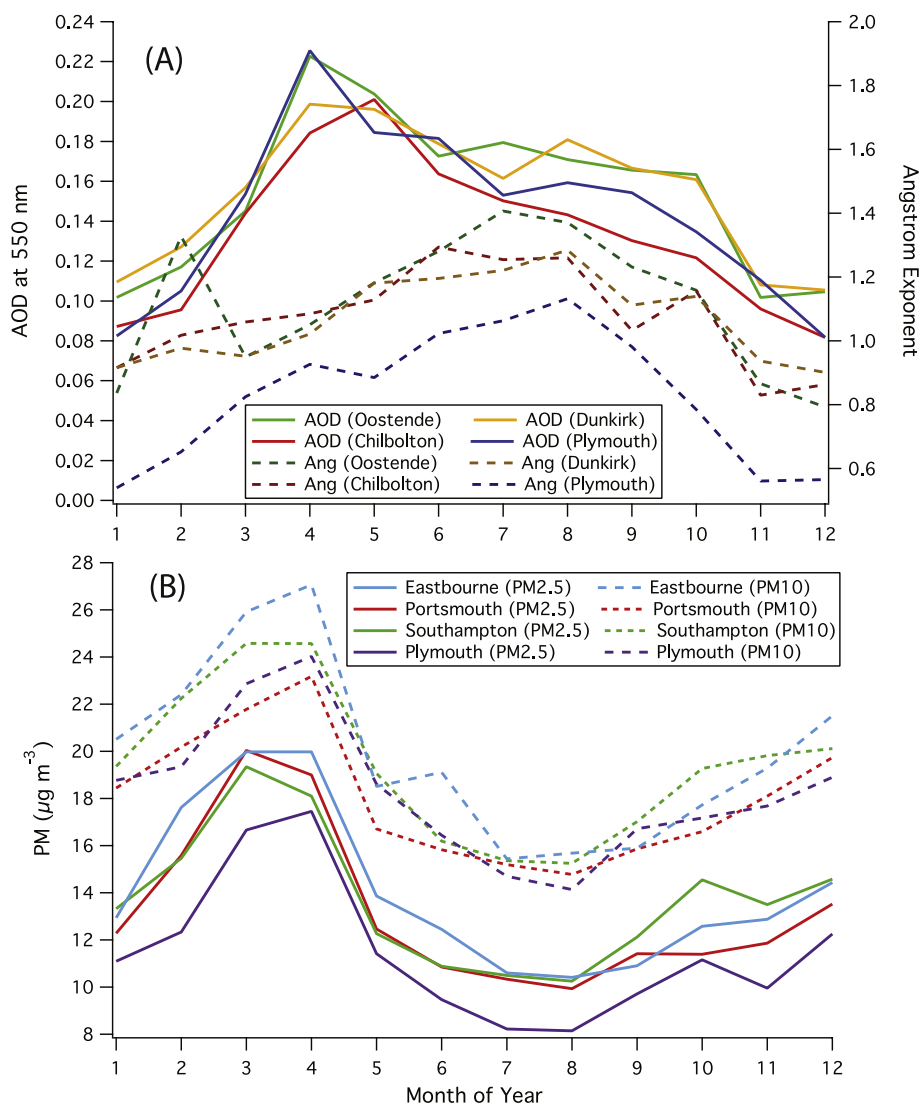


Fig. 4. Seasonal variation in (A) AOD at 550 nm and Ångström exponent at all sun photometer sites, data from the early 2000s to ~2016, and (B) PM_{2.5} and PM₁₀ from the DEFRA sites, data from 2010 to 2017.

(November to February), and then compute the respective means for each year. For the PM measurements, which are affected by PBL height changes, we focus on early spring (March to April) and winter (November to February). These choices are guided by the averaged seasonality shown in Fig. 4.

The fastest decrease in AOD is observed in the spring/early summer at approximately twice the annual rate, whilst the wintertime trends at most sites are insignificant (Table 1). The rates of decrease in PM_{2.5} in early spring are about 3–4 times faster than the annual rates in Portsmouth, Southampton, and Eastbourne (Table 2). These results demonstrate an increasingly damped seasonality in the small aerosols, which is largely due to the decreases in high aerosol concentrations that occur most often in the spring/early summer. The long-term decreasing trend in small aerosols is also mostly driven by this spring/early summer time reduction. In contrast, reductions in the seasonal amplitude as well as in the springtime peaks of PM₁₀ are less significant.

3.3. Plymouth AOD, PM, and their relationship

Plymouth, the westernmost of the sites analyzed here, is well exposed to air coming off the Atlantic Ocean. Average aerosol loading in Plymouth between 2010 and 2016 strongly depends on the local wind direction (Fig. 5). AOD at 400 nm and PM both peak when winds are

from the east (90°). In contrast, winds from the west (270°) are characterized by aerosol loadings that are lower by a factor of ~3. AOD at 1020 nm does not peak during easterly conditions, but instead shows similar values to AOD at 400 nm during westerly conditions. PM₁₀ also shows a secondary peak when winds are from the west. These observations are likely due to the contributions of sea spray to the overall aerosol loading in Plymouth (Section 4.2).

To isolate the role of small aerosols (more dominated by anthropogenic pollution), we take the difference in AOD between 400 nm and 1020 nm ($\Delta\text{AOD} = \text{AOD}_{400} - \text{AOD}_{1020}$). There is a high degree of correlation between total PM_{2.5} and ΔAOD in wind direction bins (R^2 of 0.84), with a slope of about $120 \mu\text{g m}^{-3} \Delta\text{AOD}^{-1}$ and an intercept near zero (Fig. 6). Without subtracting AOD₁₀₂₀ first, the R^2 value between AOD at 400 (500) nm and PM_{2.5} is lower at 0.70 (0.60), with a slope of 94 (116) $\mu\text{g m}^{-3} \text{AOD}^{-1}$. These PM:AOD relationships are higher than previously calculated relationships by e.g. Kacenenbogen et al. (2006) and Shao et al. (2017), and within range of findings by Schaap et al. (2009) and Xin et al. (2016).

We remind readers here that the AOD measurement is only possible in the daytime and during largely cloud free conditions. The PM measurement, on the other hand, is continuous. In deriving the above mean PM:AOD relationship, we did not restrict the PM data to only the hours of valid AOD measurements. Such a filter would lead to an averaged

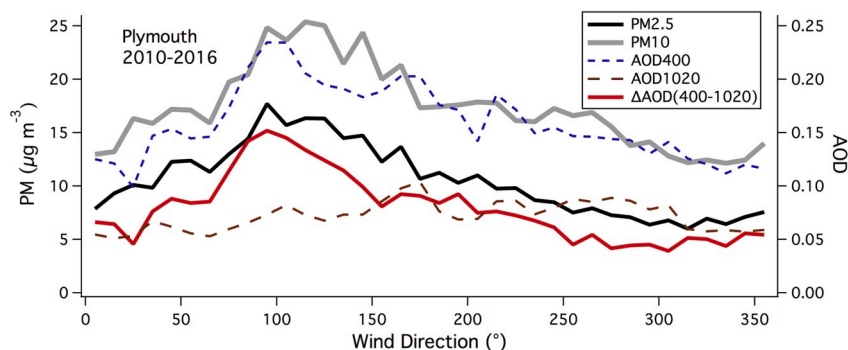


Fig. 5. Wind direction dependence in AOD (400 and 1020 nm, and their difference Δ AOD) and PM (PM2.5 and PM10) in Plymouth (averaged data from 2010 to 2016).

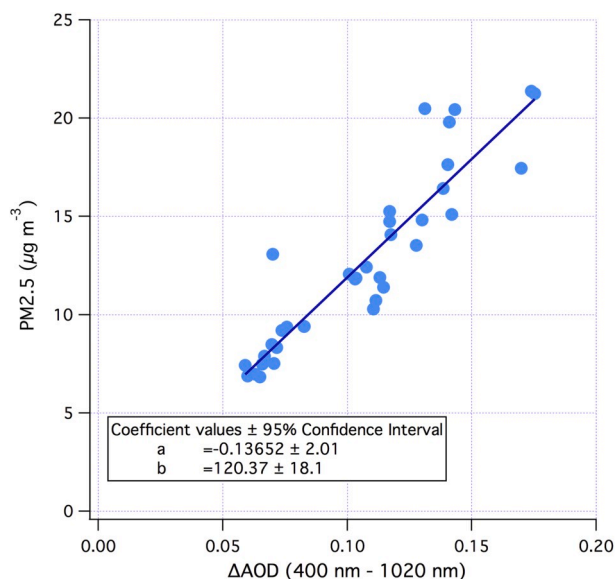


Fig. 6. Plymouth PM2.5 in wind direction bins highly correlates with Δ AOD ($r^2 = 0.84$), with a slope of $120 \mu\text{g}/\text{m}^3/\Delta$ AOD and an intercept of nearly 0.

PM2.5 concentration that is about 4% higher than the overall measured mean for Plymouth, likely due to effects such as diurnal variability and wet deposition removal. In general, we expect relationships between PM2.5 and AOD to depend on aerosol composition, size distribution, as well as seasonality, and thus not be universal. Furthermore, the empirical ratio between PM2.5 and Δ AOD (AOD400-1020) above encompasses all seasons, and is likely more suitable for relating long-term (e.g. annual) averages than for converting short-term (e.g. hourly) measurements. Assuming the summertime minima in PM is primarily due to a deepening PBL, we would expect our mean PM2.5: Δ AOD relationship to overestimate PM2.5 (from AOD data) in the summer and underestimate PM2.5 during the rest of the year.

3.4. Dependence on wind direction and spatial variability

The seasonal analysis above highlighted spatial variability in the aerosol loading along the English Channel. Fig. 7 illustrates the wind direction dependence in PM2.5, Δ AOD, and Ångström exponent at all sun photometer sites. We see that winds from the east are associated with the highest PM2.5, Δ AOD, and Ångström exponent (i.e. proportionally more small aerosols). In contrast, the lowest loading of small aerosols is found in the west/southwest wind sector, consistent with reduced pollution in marine air. Figs. 7B and 4aA show that on average, the eastern sites Dunkirk and Oostende have higher AOD (by 0.02–0.03

in the mean) than the westernmost site of Plymouth.

We use the relationship between PM2.5 and Δ AOD from Plymouth to crudely approximate PM2.5 at the other sun photometer sites for the period of August 2010 to July 2016. The estimated mean PM2.5 concentrations at Chilbolton, Dunkirk, and Oostende are shown alongside in situ PM2.5 measurements in Fig. 8. An increasing trend in PM2.5 from Plymouth eastwards is clear, with a slope of about $0.007 \mu\text{g m}^{-3} \text{ km}^{-1}$. PM2.5 in Plymouth is more than $1 \mu\text{g m}^{-3}$ lower in the mean than in Portsmouth, despite the fact that these two cities have similar PM10 levels (Table 2 and Fig. 8). The spatial trend in PM10 is less obvious than that in PM2.5, probably because PM10 is more related to aerosols of local origin.

In situ PM2.5 measurements from two ATMO surface sites in Dunkirk are also shown in Fig. 8. These two urban background stations (DK4, $51^\circ 2' 55'' \text{ N}$, $2^\circ 25' 12'' \text{ E}$; DKH, $50^\circ 59' 46'' \text{ N}$, $2^\circ 21' 59'' \text{ E}$) are each about 4 km from the sun photometer site in Dunkirk ($51^\circ 2' 6'' \text{ N}$, $2^\circ 22' 5'' \text{ E}$). The DKH measurement of PM2.5 is very close to the indirect estimate from AOD, while the DK4 site closer to the coast had lower PM2.5. The reasonable agreement between the estimated PM2.5 (from AOD) and the in situ measurements confirm the robustness of the PM2.5 and Δ AOD relationship.

4. Discussion

We have shown so far that aerosols near the English Channel display clear long-term trends as well as seasonal and spatial variability. The seasonality in aerosol loading over Europe has been the subject of a number of studies. The higher loading in the warmer months has been associated with seasonal changes in the wind patterns and precipitation (e.g. Chubarova, 2009), increased biogenic (both terrestrial and marine) precursor gas emissions (e.g. Andreae and Crutzen, 1997), more active oxidative chemistry (e.g. Chubarova, 2009), and episodically to biomass burning (Zdun et al., 2011) and long-distance transport of mineral dust (e.g. Estellés et al., 2012b; Zhao et al., 2018). In this section, we look at the influences of anthropogenic emissions (Section 4.1), sea spray production (Section 4.2), and regional weather patterns (Section 4.3) on the temporal and spatial trends of aerosols.

4.1. Impact of anthropogenic emissions on the aerosol trends

The relative reductions in AOD (from the early 2000s to ~2016) and in PM2.5 (from 2010 to 2017) are on the order of 23% and 44% decade⁻¹, respectively. We showed in Section 3.2 that the long-term decrease in the annual mean aerosol loading is largely driven by the large reduction near the spring (Tables 1 and 2). We showed in Section 3.4 that there is a general increase in the loading of small aerosols from west to east along the English Channel, and the aerosol loading tends to peak when winds are from the east. A reduction in AOD over Western Europe has been reported by several authors already (de Meij et al., 2012; Mao et al.,

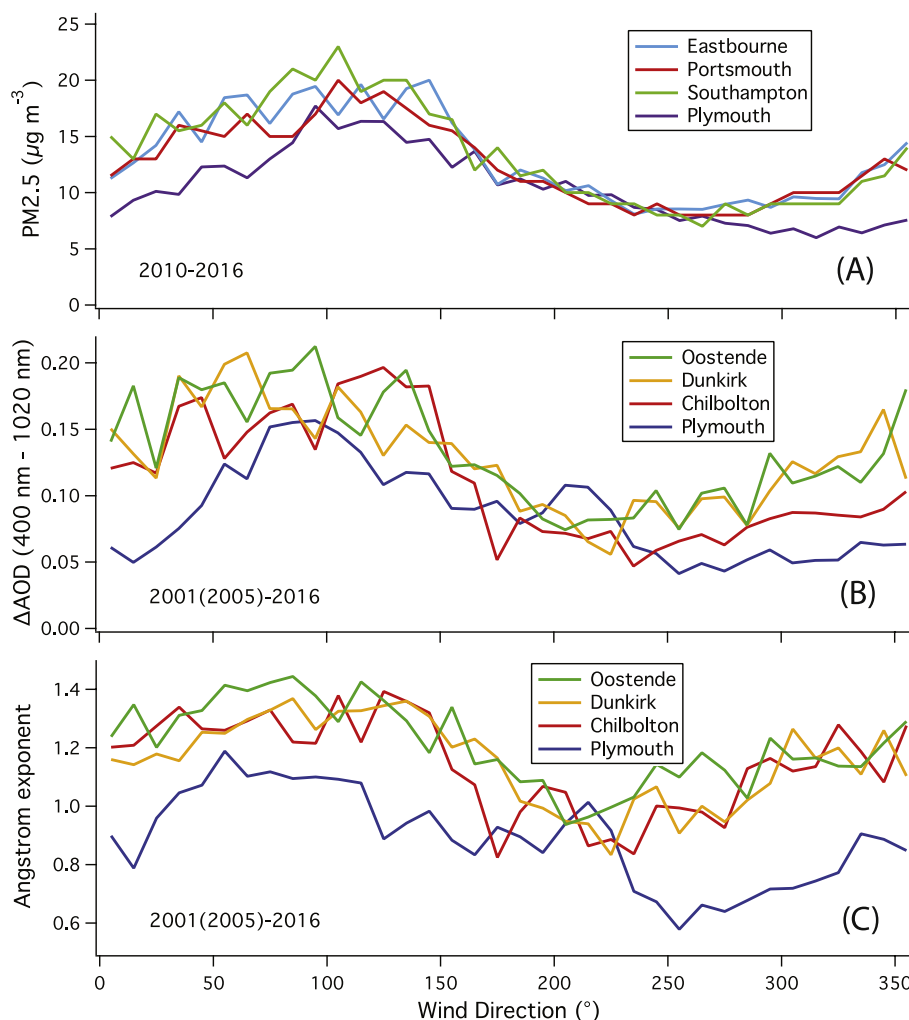


Fig. 7. Wind direction dependence in PM_{2.5} (A), DAOD (B), and Ångström exponent (C) at all sun photometer sites.

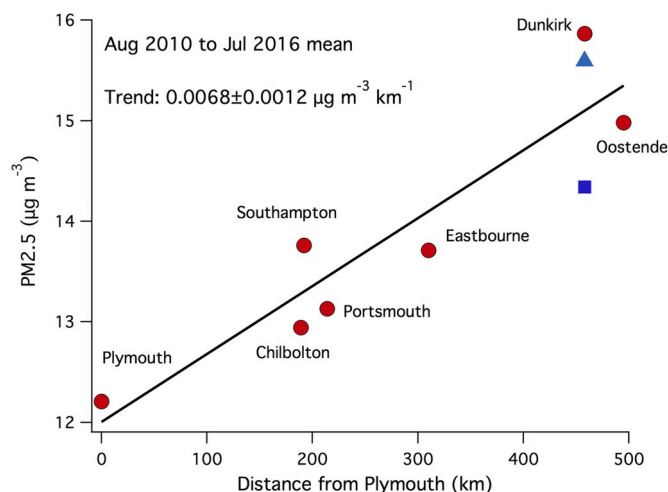


Fig. 8. Mean PM_{2.5} (2010–2016) increases with distance from Plymouth. Values from Chilbolton and Oostende were estimated from AOD, while values from Plymouth, Southampton, Portsmouth, and Eastbourne were directly measured. For Dunkirk, the red circle was estimated from AOD, while the light blue triangle and dark blue square were directly measured from the DKH and DK4 sites, respectively (see main text for further details). (For interpretation of the references to colour in this figure legend, the reader is referred to the Web version of this article.)

2014; Yoon et al., 2016; Zhao et al., 2017; Ningombam et al., 2019), and has been generally attributed to a decrease in the emission of aerosol precursors in Europe. Here we briefly examine the trends in the emissions of different precursor compounds in relation to the aerosols.

According to European Environmental Agency (<https://www.eea.europa.eu/data-and-maps/indicators/main-anthropogenic-air-pollutant-emissions/assessment-5>), from 2001 to 2015, anthropogenic emissions of nitrogen oxides (NO_x) decreased from 12.8 to 7.8 Tg yr⁻¹ (39% decade⁻¹), sulfur oxides (SO_x) decreased from 11.6 to 4.8 Tg yr⁻¹ (60% decade⁻¹), non-methane volatile organic carbon (NMVOC) decreased from 10.4 to 6.6 Tg yr⁻¹ (35% decade⁻¹), and primary PM_{2.5} decreased from 1.7 to 1.3 Tg yr⁻¹ (18% decade⁻¹). In contrast, ammonia emission has stayed around 5 Tg yr⁻¹ over these years. The bulk of these emissions occurs over the European continent.

Amongst the aerosol precursor gases, the decrease in the SO_x (mostly SO₂) emission in Europe has been the most dramatic. Given the high conversion efficiency from SO_x to sulfate aerosols, the reduction in SO_x likely contributed significantly to the decreasing trend in aerosols (Tørseth et al., 2012). Aerosol sulfate is primarily found in the sub-micron mode (e.g. Yang et al., 2011), and less sulfate is expected to result in proportionally lower fine aerosol mass. Indeed, in Eastbourne, Portsmouth, and Southampton the PM_{2.5}:PM₁₀ ratio has decreased by similar amounts, from approximately 0.75 in 2010 to 0.62 in 2017.

Interestingly a trend in the Ångström exponent is not obvious at any of the four sun photometer sites (Table 1), in contrast to the findings from Zhao et al. (2017) based on satellite observations. A consistent

long-term trend in the single scatter albedo is also not apparent among the sun photometer sites (supplement Fig. S2). These observations suggest that the reduction of aerosols along the English Channel is not limited to highly scattering particulates in the submicron mode (e.g. sulfate). Both organics (oxidation products of NMVOC) and nitrate (products of NO_x and ammonia) are often found in both the fine mode and coarse mode of aerosols (e.g. Kavouras and Stephanou, 2002; Yeatman et al., 2001). Considering their larger present day emissions than SO_x and the slower rates of reductions that are more comparable to those of aerosol loading, NMVOC and NO_x appear to be also important for the aerosol trends and present day composition.

Road transport is the largest source of NO_x in Europe but produces relatively low amounts of NMVOC and SO_x . In addition to NO_x and soot carbon, road transport also generates primary aerosols from brake and tyre wear, as well as resuspension of pre-existing aerosols (Thorpe and Harrison, 2008). Our crude analyses of the weekday-weekend difference below show that traffic is clearly a significant source of aerosols at these sites, but does not appear to be a major contributor towards the long-term aerosol trend.

Averaged PM shows that PM2.5 peaks on Thursdays at all sites in the mean, and decrease towards the weekend (supplement Fig. S3). Averaged AOD also tends to peak on Thursdays or Fridays (supplement Fig. S4). The average weekday-weekend difference in PM2.5 in Eastbourne, Plymouth, Portsmouth, Southampton amounts to 1%, 4%, 5%, and 7%, respectively (mean of 4% across all sites, or about $0.5 \mu\text{g m}^{-3}$). The weekday-weekend difference in AOD (550 nm) is about 2%, 4%, 7%, and 10% in Plymouth, Chilbolton, Oostende, and Dunkirk, respectively (mean of 6% across all sites, or 0.009 in AOD). Here for simplicity, we categorize 'weekdays' as Tuesday to Friday, and 'weekend' as Saturday to Monday. Assigning Mondays as 'weekends' here very roughly recognizes the fact that aerosol loadings tend to be low before the Monday morning traffic and also attempts to account for the time needed for secondary aerosol formation.

According to the UK Department of Transport, the average weekday-weekend difference in vehicle traffic volume is about 25% (<https://www.gov.uk/government/statistics/road-traffic-estimates-in-great-britain-2013>). Assuming the weekday-weekend difference in aerosols at all sites is due to the difference in traffic volume alone (i.e. 25%), the total contribution of traffic towards PM2.5 and AOD (550 nm) would be on the order of $2.1 \mu\text{g m}^{-3}$ and 0.034, respectively (~20% of the PM2.5 and AOD at these locations). The weekday-weekend differences in PM2.5 and in AOD (averaged to yearly bins) do not show significant long-term trends at any of the sites here, suggesting limited changes in overall road traffic emissions. This may be because while the per-vehicle NO_x emissions has reduced over the last two decades (especially for petrol vehicles), the total road traffic volume in Europe has increased (<https://www.eea.europa.eu/signals/signals-2016/articles/transport-in-europe-key-facts-trends>).

With regard to the shipping industry, the maximum allowed fuel sulfur content within the Sulfur Emission Controlled Areas (including the English Channel) has reduced from 1.5% (pre-July 2010), to 1% (post-July 2010), to 0.1% (post-January 2015). A step-wise reduction in aerosol loading due to ship emission regulations is not obvious in the AOD as well as PM data at the sites analyzed here. In Plymouth and Dunkirk, the two sites with relatively few gaps in the sun photometer data, AOD (550 nm) was actually higher from July 2010 to June 2011 than from July 2009 to June 2010 by approximately 0.02. AOD in calendar year 2015 was about 0.01–0.02 lower than in calendar year 2014 at these two sites. But this difference is within the interannual variability of about 0.02 at these locations (Section 3.1). Averaged across the DEFRA surface sites, the mean PM2.5 in calendar years 2015 and 2016 was on average $\sim 0.3 \mu\text{g m}^{-3}$ lower than in 2014, with reductions more obvious in Portsmouth and Southampton than in Plymouth and Eastbourne. However, as with AOD, this difference is within the interannual variability in PM2.5 of 0.9–2.0 $\mu\text{g m}^{-3}$.

The IMO ship sulfur emission regulations have probably reduced

aerosol loadings at these coastal sites, which are however obscured by other sources of variability. That the shipping regulations have not led to more obvious reductions in AOD and PM2.5 after 2015 is probably because the SO_x emissions within these SECA zone were already fairly low. The total SO_x emission due to shipping in Europe was estimated to be 1.2 Tg yr^{-1} for the year 2011 (Jalkanen et al., 2016). A 3-fold reduction (see Yang et al., 2016) would lead to a reduction in ship SO_x emission of about 0.8 Tg yr^{-1} from pre-to post-2015. This is of the same magnitude as the average annual decrease in total European SO_x emission ($\sim 0.5 \text{ Tg yr}^{-1}$) during this period. We note that ship emissions are likely more important for the budgets of coastal aerosol number and Aitken mode aerosol mass than for PM2.5, PM10, or AOD (Kivekäs et al., 2014).

4.2. Sea spray contribution to aerosol budget

The presence of sea spray aerosols is clearly evident at these coastal sites, and especially pronounced in Plymouth. To estimate the sea spray contribution towards AOD and PM, we look at their wind speed dependencies. Fig. 9 shows the wind speed dependence of AOD from 400 and 1020 nm in Plymouth (data averaged from 2001 to 2016). Here we restrict our data to the southwest direction (190 to 260°) that faces the North Atlantic. At wind speeds over 10 ms^{-1} , AOD at all wavelengths increases whilst the Ångström exponent trends towards zero. At low wind speeds ($< 4 \text{ ms}^{-1}$), elevated AOD values are also observed (more pronounced at 400 nm than at 1020 nm), which are most likely due to local pollution.

Mulcahy et al. (2008) reported AOD observations from Mace Head, Ireland using a Precision Filter Radiometer. They identified a strong wind speed dependence in AOD that was attributed to sea spray after selecting their data for periods of clean marine air (based on local wind direction, black carbon, aerosol number concentration, and airmass back trajectory). Their AOD vs. wind speed relationship are also shown in Fig. 9 at 500 and at 862 nm, which are very similar to each other because there is little wavelength dependence in the AOD of sea spray aerosols. These empirical fits for sea spray are fairly close to the Plymouth observations at moderate wind speeds and a slight overestimate at high wind speeds. At very low wind speeds, there is a small, non-zero intercept of about 0.06 in AOD500 in the Mulcahy et al. (2008) parameterization, which could be due to sea spray aerosols generated from swell (instead of local wind waves) or due to marine aerosols produced further upwind.

To estimate the contribution of sea spray towards AOD on a seasonal scale, we use the wind speed dependent Mulcahy et al. (2008) parameterization. The result of this calculation for Plymouth is shown both for southwest wind sector (190 to 260°) only and for all wind directions in the supplement Fig. S5. During southwesterly conditions, the sea spray fraction of AOD at 500 nm varies from about 40% in summer to 70% in winter (annual average of 56%). With respect to all wind directions, sea spray accounts for an AOD of about 0.02 at 500 nm, or 16% of the total AOD in Plymouth. The proportional contribution of sea spray to total AOD is greater at longer wavelengths (20% at 870 nm) and less at shorter wavelengths (13% at 400 nm). If we conservatively consider the non-zero intercept in the Mulcahy et al. (2008) parameterization not to be sea spray, the overall annual sea spray contribution to AOD500 would be reduced to about 5% in Plymouth.

AOD at 1020 nm in Oostende, Dunkirk, and Chilbolton (southwest wind direction only) are lower in magnitude and show less wind speed dependence than AOD in Plymouth (Fig. 10). Sea spray constitutes a lower fraction of aerosol burden further east along the English Channel, likely because wind speeds are lower and waves are smaller, resulting in lower sea spray productions (Yang et al., 2019). However, the effect of sea spray aerosols is not negligible in Oostende, Dunkirk, and Chilbolton, as evidenced by the observed decreasing Ångström exponent with increasing wind speed.

We also estimate the sea spray contribution to PM. Here we take the

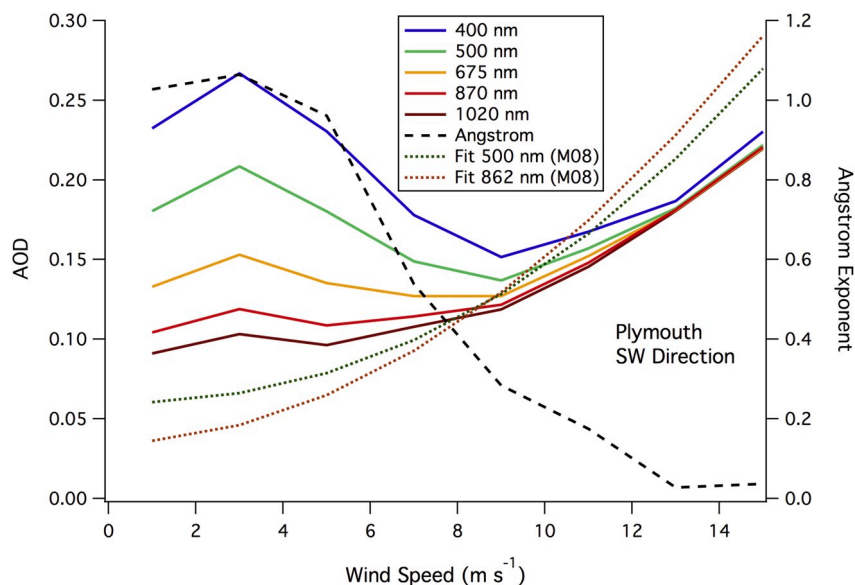


Fig. 9. AOD in Plymouth (2001 to 2016, southwest direction only) increases with wind speed, especially in the infrared, while the Ångström exponent decreases with wind speed, consistent with sea spray production. Also shown are empirical fits of AOD from Mulcahy et al., (2008) (M08) based on marine air measurements at Mace Head, which are fairly close to the PML observations at intermediate wind speeds.

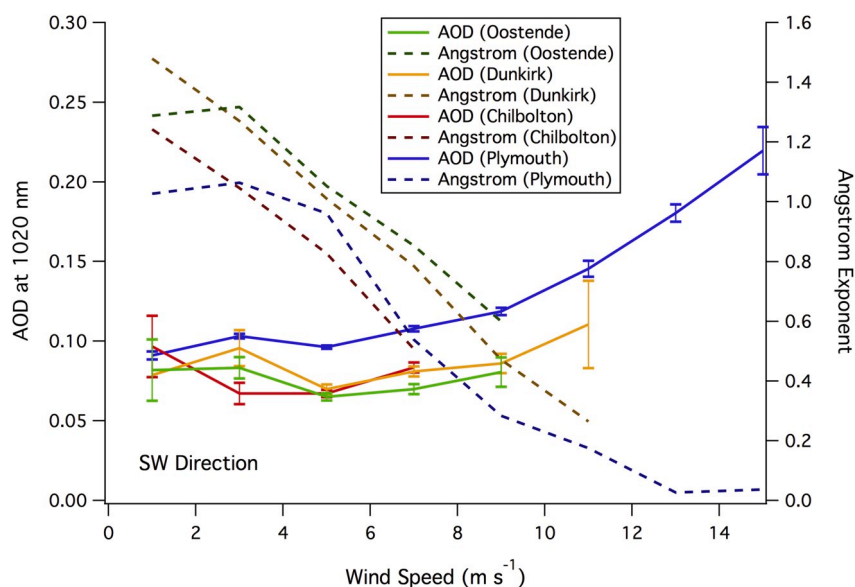


Fig. 10. AOD at 1020 nm (wavelength least sensitive to pollution) and the Ångström exponent from the four sun photometer sites (southwest wind direction only). A lower AOD and weaker wind speed dependence in AOD (by ~40%) are observed at the eastern sites compared to Plymouth, suggesting a reduced importance of sea spray.

difference between non-volatile (nv) PM10 and PM2.5 ($\Delta PM = PM_{10nv} - PM_{2.5nv}$) in order to separate the influence of local pollution from the sea spray signal. Fig. 11 shows ΔPM for the southwest direction as a function of wind speed for Plymouth, Eastbourne, Portsmouth, and Southampton. At all sites, ΔPM clearly increases with wind speed. The slope is about twice as steep in Plymouth as compared to the more eastern sites, proportionally similar to the AOD slopes in Fig. 10.

During southwesterly conditions only, the sea spray fraction of PM10 varies seasonally, increasing from about 45% in the summer to nearly 60% in the winter (mean of 49%, or $8.9 \mu g m^{-3}$). Considering all wind directions, the sea spray contribution to PM10 is about 13% ($\sim 2.3 \mu g m^{-3}$) in Plymouth (see supplement S6). For the more eastern sites of Eastbourne, Southampton, and Portsmouth, the aerosol concentration due to sea spray is approximately half as much as in Plymouth primarily due to

the weaker wind speed dependence in ΔPM .

As with AOD, there appears to be a small, non-zero intercept in ΔPM at a wind speed of zero (about $5 \mu g m^{-3}$ in Plymouth). If we conservatively assume that this non-zero intercept in ΔPM is not sea spray, the sea spray contribution to PM10 in Plymouth would reduce to ~6% ($1 \mu g m^{-3}$) on an annual average. Note that in the PM analysis, we are unable to estimate the sea spray contribution towards PM2.5. The few direct measurements of sea spray aerosol flux (e.g. Norris et al., 2013) suggests that 10–20% of the total sea spray mass flux exists at a diameter less than $2.5 \mu m$. Because of their smaller size and thus lower rates of deposition, these sea spray aerosols are expected to have a longer atmospheric lifetime and contribute more to the PM2.5 burden further inland than the larger sea spray aerosols.

In summary, the contribution of sea spray towards the overall aerosol

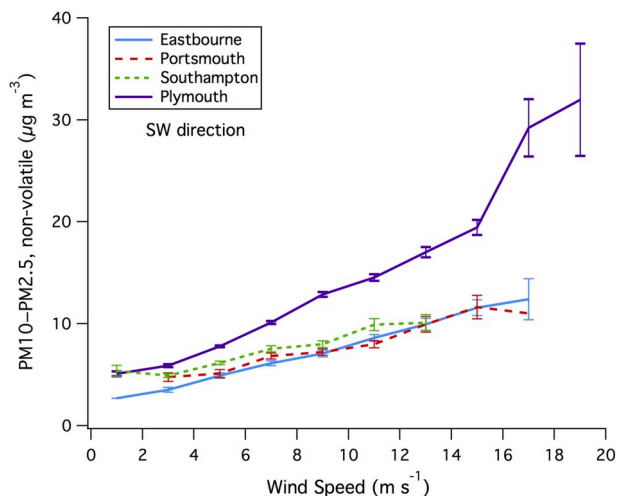


Fig. 11. Difference between non-volatile PM10 and PM2.5 (ΔPM) vs. wind speed for all DEFRA sites (southwest direction only). Error bars denote standard errors. At all sites, delta PM clearly increases with wind speed, consistent with sea spray formation (e.g. r^2 of 0.9 in Plymouth). ΔPM for Eastbourne, Portsmouth and Southampton show slopes against wind speed that are about half as steep as what is observed in Plymouth, consistent with less sea spray further east along the English Channel.

loading is modest overall, with decreasing importance from west to east. There can be substantial sea spray aerosols during southwesterly conditions that are more prevalent in the wintertime (which does not explain the peak AOD and PM around the spring). Even with additional sea spray contributing towards the total aerosol loading, marine air still tends to have a lower AOD and PM2.5 compared to the more polluted continental air (Fig. 7). A consistent long-term decrease in wind speed is not observed at these coastal sites. Thus the long-term reduction in aerosol loading is unlikely to be due to changes in sea spray production.

4.3. The roles of circulation and natural variability

Given the importance of wind direction and seasons on AOD and PM, aerosols along the English Channel may be sensitive indicators of changes in the regional and/or North Atlantic weather patterns. To

assess regional meteorological effects on the aerosols, we look at the local surface winds, relative humidity (RH), and rain rate. For the four sun photometer sites, we convert the local wind speed and direction into their vector components: zonal (+from W to E) and meridional (+from S to N) wind velocities. The mean seasonality of these velocities (data from 2001 to 2016) is shown in Fig. 12. Being in the mid-latitudes, the mean wind flows at all sites are unsurprisingly from west to east. However, the springtime, and to a lesser degree the autumn, is characterized by the lowest mean W to E flow (or more low wind conditions/easterlies). It is these stagnant conditions/easterly winds that tend to result in the highest aerosol loading near the English Channel. We note that RH and rain rate are at their lowest of the year during April/May also (see supplement Fig. S7). Reduced wet deposition of aerosols and precursor gases likely contribute to the build-up of aerosols during these dry periods.

We look at the North Atlantic Oscillation (NAO) index to assess the importance of transport and inter-decadal variability over the North Atlantic on the aerosol trends. The NAO, computed from the pressure difference between Iceland and Azores/Gibraltar, tends to be positive in winter when there are stronger than usual westerly winds over the Atlantic (Jones et al., 1997; Osborn, 2011). A positive NAO should result in a greater degree of maritime influence (e.g. more precipitation at higher latitudes, Hurrell, 1995, and more sea spray production) as well as more transport of pollutants from North America across the Atlantic (Christoudias et al., 2012). A negative NAO tends to be associated with calmer and dryer weather over Northern Europe. Reduced westerlies favor more accumulation and outflow of pollutants emitted from continental Europe (Christoudias et al., 2012).

There appears to be an anti-correlation between AOD and NAO seasonally. This is perhaps most obvious on a monthly time scale at Dunkirk, the sun photometer site with the fewest data gaps (Fig. 13). Some of the very positive NAO events (e.g. winters of 2006/2007, 2011/2012, 2013/2014) corresponded to very low AODs. Conversely, some of the negative NAO events (e.g. May 2013 and June 2014) were associated with quite high AODs. Seasonally averaged, the mean NAO is positive in winter, corresponding to generally low aerosol loading (Fig. 4). NAO tends to be close to zero or negative in the warmer months, which is associated with higher loadings of aerosols. These results show that accumulation/outflow of pollutants emitted from continental Europe is a more important driver for the spring-time AOD peak near the English Channel than trans-Atlantic transport of North American pollutants and

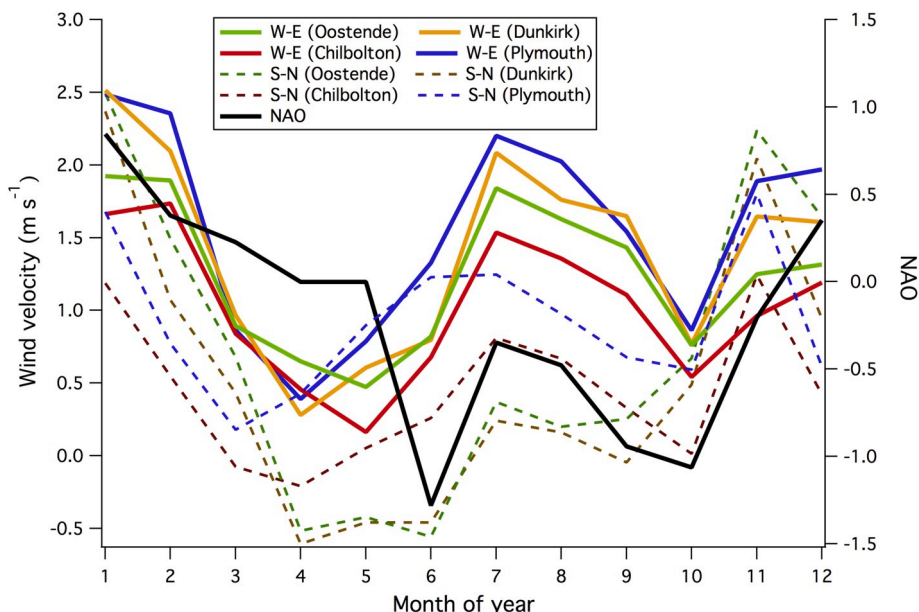


Fig. 12. Seasonal cycle in zonal (+from W to E), meridional (+from S to N) wind velocities, and the North Atlantic Oscillation index averaged from 2001 to 2016.

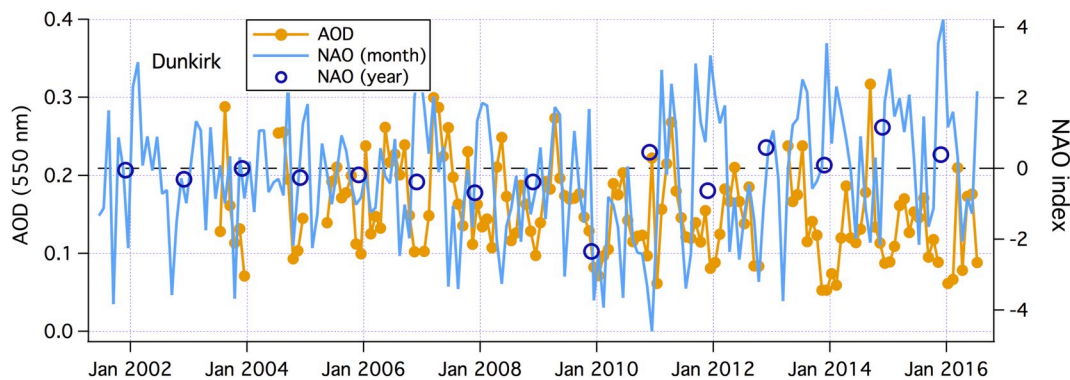


Fig. 13. Monthly times series of AOD at Dunkirk and the NAO index.

sea spray production. This seasonality in the flow patterns is an important reason why the long-term reduction in aerosol loading is most obvious during the springtime, and less obvious in winter.

How much of the long-term trends in AOD is due to change in the large-scale circulation? We see that as annual averages, the first 8–9 years of this 15-year time series had slightly negative NAO, with the winter of 2009/2010 being especially negative. The last 5–6 years of this record had a more positive NAO. Annual mean AOD at the four sun photometer sites, whether with the long-term trend removed or not, correlate very weakly with the NAO (see supplement Figs. S8 and S9). Furthermore we find no significant long-term trend in the zonal wind velocities, precipitation, and relative humidity at the four sun photometer sites over the last 15 years. Thus while the transition from a negative phase in NAO to a positive phase within this 15-year time series coincided with the gradual reductions in AOD, changes in circulation and weather patterns do not appear to be the main cause for the aerosol trend from the early 2000s to ~2016. Instead, the long-term decrease in aerosols observed over Western Europe is most consistent with the reduction in European pollutant emissions.

5. Conclusions

Ground based observations clearly show that the loadings of small aerosols in coastal cities along the English Channel have decreased over the last decade and a half. From the early 2000s to about 2016, annual mean AOD decreased by an overall average of 23% decade⁻¹. From 2010 to 2017, annual mean concentration of PM_{2.5} decreased by an overall average of 44% decade⁻¹. The decreasing trend in aerosols is most pronounced around the springtime and further east along the English Channel, which is due to the interaction between the seasonal weather patterns (e.g. reduced westerly flow and drier weather around the spring/early summer) and the strong emission sources from the European Continent. There is a clear spatial gradient in the aerosol loading and in the aerosol composition. From west to east along the English Channel, PM_{2.5} concentration increases at a rate of about 0.007 $\mu\text{g m}^{-3} \text{ km}^{-1}$. Sea spray is estimated on average to account for 16% of the AOD and 13% of the PM₁₀ at the westernmost site Plymouth. The contribution of sea spray towards the total aerosol loading is reduced by about a factor of two at the more eastern sites. Overall, the long-term decrease in aerosol loading is more consistent with the reductions in anthropogenic emissions, rather than with changes in large-scale atmospheric transport such as the North Atlantic Oscillation. However, clean ups in road vehicles emissions and ship emissions do not appear to be strong drivers for the observed decrease in aerosol loading.

Data availability

All data used in this work are publically accessible. AERONET sun photometer data are available at <https://aeronet.gsfc.nasa.gov/>. The

PML POM Sun photometer data are available at www.westernchannelobservatory.org.uk/. The DEFRA Automatic Urban and Rural Network (AURN) measurements are available at <https://uk-air.defra.gov.uk/data/>. The ATMO data are available at <https://www.atmo-hdf.fr/>.

Declaration of competing interest

The authors declare that they have no known competing financial interests or personal relationships that could have appeared to influence the work reported in this paper.

CRediT authorship contribution statement

Mingxi Yang: Formal analysis, Writing - original draft. **Joelle C.E. Buxmann:** Writing - original draft. **Hervé Delbarre:** Writing - original draft. **Marc Fourmentin:** Writing - original draft. **Tim J. Smyth:** Writing - original draft.

Acknowledgement

This work was partly funded by the UK Natural Environment Research Council through its National Capability Long-term Single Centre Science Programme, Climate Linked Atlantic Sector Science, grant number NE/R015953/1, and is a contribution to Theme 4 - Fixed Point Observations (Western Channel Observatory). This work is also a contribution to the NERC project ACSIS (The North Atlantic Climate System Integrated Study, NE/N018044/1). We thank Darcy Ladd and the NERC Facility for Atmospheric and Radar Research (NFARR) for the sun photometer data at the STFC Chilbolton Observatory, and Kevin Ruddick for the sun photometer data in Oostende. We acknowledge Defra and uk-air.defra.gov.uk for the AURN surface aerosol measurements. © Crown 2019 copyright Defra via uk-air.defra.gov.uk, licenced under the Open Government Licence (OGL). Finally, we thank Tom Bell, Peter Land (Plymouth Marine Laboratory), John Bruun (University of Exeter), and Helen Wells (UK Met Office) for stimulating discussions.

Appendix A. Supplementary data

Supplementary data to this article can be found online at <https://doi.org/10.1016/j.aeoa.2020.100074>.

References

- Andreae, M.O., Crutzen, P.J., 1997. Atmospheric aerosols: biogeochemical sources and role in atmospheric chemistry. *Science* 276, 1052–1058.
- Andreas, E., 2016. Sea Spray Generation at a Rocky Shoreline. *JAMC*. <https://doi.org/10.1175/JAMC-D-15-0211.1>.
- Angal, A., Xiong, X.X., Choi, T., Chander, G., Mishra, N., Helder, D.L., 2013. Impact of Terra MODIS Collection 6 on long-term trending comparisons with Landsat 7 ETM+ reflective solar bands. *Remote Sensing Letters* 4 (9), 873–881.

- Chan, K.M., Wood, R., 2013. The seasonal cycle of planetary boundary layer depth determined using COSMIC radio occultation data. *J. Geophys. Res. Atmos.* 118 (12) <https://doi.org/10.1002/2013JD020147>, 4222–12,434.
- Christoudias, T., Pozzer, A., Lelieveld, J., 2012. Influence of The North Atlantic oscillation on air pollution transport. *Atmos. Chem. Phys.* 12, 869–877. <https://doi.org/10.5194/acp-12-869-2012>.
- Chubarova, N.Y., 2009. Seasonal distribution of aerosol properties over Europe and their impact on UV irradiance. *Atmos. Meas. Tech.* 2, 593–608. <https://doi.org/10.5194/amt-2-593-2009>.
- Curci, G., Hogrefe, C., Bianconi, R., Im, U., Balzarini, A., Baró, R., Brunner, D., Forkel, R., Giordano, L., Hirtl, M., Hozak, L., Jiménez-Guerrero, P., Knote, C., Langer, M., Makar, P.A., Pirovano, G., Pérez, J.L., San José, R., Syrakov, D., Tuccella, P., Werhahn, J., Wolke, R., Zabkar, R., Zhang, J., Galmarini, S., 2015. Uncertainties of simulated aerosol optical properties induced by assumptions on aerosol physical and chemical properties: an AQMEII-2 perspective. *Atmos. Environ.* 115, 541–552. <https://doi.org/10.1016/j.atmosenv.2014.09.009>.
- de Leeuw, G., Andreas, E.L., Anguelova, M.D., Fairall, C.W., Lewis, E.R., O'Dowd, C., Schulz, M., Schwartz, S.E., 2011. Production flux of sea spray aerosol. *Rev. Geophys.* 49, RG2001. <https://doi.org/10.1029/2010RG000349>.
- de Meij, A., Pozzer, A., Lelieveld, J., 2012. Trend analysis in aerosol optical depths and pollutant emission estimates between 2000 and 2009. *Atmos. Environ.* 51, 75–85. <https://doi.org/10.1016/j.atmosenv.2012.01.059>.
- Eck, T.F., Holben, B.N., Reid, J.S., Dubovik, O., Smirnov, A., O'Neill, N.T., Slutsker, I., Kinne, S., 1999. Wavelength dependence of the optical depth of biomass burning, urban, and desert dust aerosols. *J. Geophys. Res.* 104, 31333–31349.
- Emissions of the main air pollutants in Europe. <https://www.eea.europa.eu/data-and-maps/indicators/main-anthropogenic-air-pollutant-emissions> last access: 8 Apr 2020, published 4 Sep 2019. /assessment-6.
- Estellés, V., Campanelli, M., Smyth, T., Utrillas, M., Martínez-Lozano, J., 2012a. Evaluation of the new ESR network software for the retrieval of direct sun products from CIMEL CE318 and PREDE POM01 sun-sky radiometers. *Atmos. Chem. Phys.* 12, 11619–11630. <https://doi.org/10.5194/acp-12-11619-2012>.
- Estellés, V., Smyth, T.J., Campanelli, M., 2012b. Columnar aerosol properties in a Northeastern Atlantic site (Plymouth, United Kingdom) by means of ground based skyradiometer data during years 2000–2008. *Atmos. Environ.* 61, 180–188. <https://doi.org/10.1016/j.atmosenv.2012.07.024>.
- Glantz, P., Freud, E., Johansson, C., Noone, K.J., Tesche, M., 2019. Trends in MODIS and AERONET derived aerosol optical thickness over Northern Europe. *Journal, Tellus B: Chem. Phys. Meteorol.* 71.
- Holben, B.N., Eck, T.F., Slutsker, I., Tanre, D., Buis, J.P., Setzer, A., Vermote, E., Reagan, J.A., Kaufman, Y.J., Nakajima, T., Lavenue, F., Jankowiak, I., Smirnov, A., 1998. AERONET – a federated instrument network and data archive for aerosol characterization. *Remote Sens. Environ.* 66 (1–16).
- Hurrell, J.W., 1995. Decadal trends in The North Atlantic oscillation: regional temperatures and precipitation. *Science* 269, 676–679.
- Jalkanen, J.P., Johansson, L., Kukkonen, J., 2016. A comprehensive inventory of ship traffic exhaust emissions in the European sea areas in 2011. *Atmos. Chem. Phys.* 16, 71–84.
- Johansson, L., Jalkanen, J.-P., Kukkonen, J., 2017. Global assessment of shipping emissions in 2015 on a high spatial and temporal resolution. *Atmos. Environ.* 167, 403–415.
- Jones, P.D., Jónsson, T., Wheeler, D., 1997. Extension to the North Atlantic Oscillation using early instrumental pressure observations from Gibraltar and South-West Iceland. *Int. J. Climatol.* 17, 1433–1450.
- Kacenenbogen, M., Leon, J.-F., Chiappello, I., Tanre, D., 2006. Characterization of aerosol pollution events in France using groundbased and POLDER-2 satellite data. *Atmos. Chem. Phys.* 6, 4843–4849. <http://www.atmos-chem-phys.net/6/4843/2006/>.
- Kavouras, I.G., Stephanou, E.G., 2002. Particle size distribution of organic primary and secondary aerosol constituents in urban, background marine, and forest atmosphere. *J. Geophys. Res.* 107 (D8) <https://doi.org/10.1029/2000JD000278>.
- Kivekäs, N., Massling, A., Grythe, H., Lange, R., Rusnak, V., Carreno, S., Skov, H., Kivietlicki, E., Nguyen, Q.T., Glasius, M., Kristensson, A., 2014. Contribution of ship traffic to aerosol particle concentrations downwind of a major shipping lane. *Atmos. Chem. Phys.* 14, 8255–8267. <https://doi.org/10.5194/acp-14-8255-2014>.
- Kristiansen, N.I., Stohl, A., Olivieri, D.J.L., Croft, B., Søvdé, O.A., Klein, H., Christoudias, T., Kunkel, D., Leadbetter, S.J., Lee, Y.H., Zhang, K., Tsigaridis, K., Bergman, T., Evangelou, N., Wang, H., Ma, P.-L., Easter, R.C., Rasch, P.J., Liu, X., Pitari, G., Di Genova, G., Zhao, S.Y., Balkanski, Y., Bauer, S.E., Faluvegi, G.S., Kokkola, H., Martin, R.V., Pierce, J.R., Schulz, M., Shindell, D., Tost, H., Zhang, H., 2016. Evaluation of observed and modelled aerosol lifetimes using radioactive tracers of opportunity and an ensemble of 19 global models. *Atmos. Chem. Phys.* 16, 3525–3561. <https://doi.org/10.5194/acp16-3525-2016>.
- Lelieveld, J., Evans, J., Fnais, M., Giannadaki, D., Pozzer, A., 2017. The contribution of outdoor air pollution sources to premature mortality on a global scale. *Nature* 525 (7569), 367–371. <https://doi.org/10.1038/nature15371>.
- Lewis, E., Schwartz, S.E., 2004. *Sea Salt Aerosol Production: Mechanisms, Methods, Measurements and Models—A Critical Review*. American Geophysical Union, Washington, DC).
- Mao, K.B., Ma, Y., Xia, L., Chen, W.Y., Shen, X.Y., He, T.J., Xu, T.R., 2014. Global aerosol change in the last decade: an analysis based on MODIS data. *Atmos. Environ.* 94, 680–6.
- Mehta, M., et al., 2016. Recent global aerosol optical depth variations and trends — a comparative study using MODIS and MISR level 3 datasets. *Rem. Sens. Environ.* 181, 137–150. <https://doi.org/10.1016/j.rse.2016.04.004>.
- Monahan, E.C., Spiel, D.E., Davidson, K.L., 1986. A model of marine aerosol generation via whitecaps and wave disruption. In: Monahan, E.C., Mac Niocaill, G., Reidel, D. (Eds.), *Oceanic Whitecaps and Their Role in Air–Sea Exchange Processes*, pp. 167–174.
- Mulcahy, J.P., O'Dowd, C.D., Jennings, S.G., Ceburnis, D., 2008. Significant enhancement of aerosol optical depth in marine air under high wind conditions. *Geophys. Res. Lett.* 35, L16810. <https://doi.org/10.1029/2008GL034303>.
- Ningombam, S.S., Larson, E.J.L., Dumkad, U.C., Estelles, V., Campanelli, M., Colwell, S., 2019. Long-term (1995–2018) aerosol optical depth derived using ground based AERONET and SKYNET measurements from aerosol aged-background sites. *Atmos. Pollut. Res.* 10 (2), 608–620.
- Norris, S.J., Brooks, I.M., Moat, B.I., Yelland, M.J., de Leeuw, G., Pascal, R.W., Brooks, B., 2013. Near-surface measurements of sea spray aerosol production over whitecaps in the open ocean. *Ocean Sci.* 9, 133–145. <https://doi.org/10.5194/os-9-133-2013>.
- Osborn, T.J., 2011. Winter 2009/2010 temperatures and a record-breaking North Atlantic Oscillation index. *Weather* 66, 19–21.
- Pope, C.A., Ezzati, M., Dockery, D.W., 2009. Fine-particulate air pollution and life expectancy in the United States, new. *Egl. J. Med.* 360, 376–386. <https://doi.org/10.1056/NEJMsa0805646>.
- Schaap, M., Apituley, A., Timmermans, R.M.A., Koelmeijer, R.B.A., de Leeuw, G., 2009. Exploring the relation between aerosol optical depth and PM2.5 at Cabauw, The Netherlands. *Atmos. Chem. Phys.* 9, 909–925. <https://doi.org/10.5194/acp-9-909-2009>.
- Seinfeld, J.H., Pandis, S.N., 2006. *Atmospheric chemistry and physics: from air pollution to climate change*, 2nd ed. Wiley-Interscience, Hoboken, New Jersey, USA.
- Shao, P., Xin, J., An, J., Kong, L., Wang, B., Wang, J., Wang, Y., Wu, D., 2017. The empirical relationship between PM2.5 and AOD in nanjing of the yangtze river delta. *Atmos. Pollut. Res.* 8 (2), 233–243. <https://doi.org/10.1016/j.apr.2016.09.001>.
- Smirnov, A., Holben, B.N., Eck, T.F., Dubovik, O., Slutsker, I., 2000. *Remote Sens. Environ.* 73, 337–349.
- Sun, J., Madhavan, S., Xiong, X., Wang, M., 2015. Long-term drift induced by the electronic crosstalk in Terra MODIS Band 29. *JGR Atmospheres* 120 (19), 9944–9954. <https://doi.org/10.1002/2015JD023602>.
- Thorpe, A., Harrison, R.M., 2008. Sources and properties of non-exhaust particulate matter from road traffic: a review. *Sci. Total Environ.* 400, 270–282.
- Tørseth, K., Aas, W., Breivik, K., Fjæraa, A.M., Fiebig, M., Hjellbrekke, A.G., Lund Myhre, C., Solberg, S., Yttri, K.E., 2012. Introduction to the European Monitoring and Evaluation Programme (EMEP) and observed atmospheric composition change during 1972–2009. *Atmos. Chem. Phys.* 12, 5447–5481. <https://doi.org/10.5194/acp-12-5447-2012>.
- van Eijk, A.M.J., Kusmierczyk-Michulec, J.T., Franciscus, M.J., Tedeschi, G., Piazzola, J., Merritt, D.L., Fontana, J.D., 2011. Sea-spray aerosol particles generated in the surf zone. *J. Geophys. Res.* 116, D19210. <https://doi.org/10.1029/2011JD015602>.
- Wang, X., Deane, G.B., Moore, K.A., Ryder, O.S., Stokes, M.D., Beall, C.M., Collins, D.B., Santander, M.V., Burrows, S.M., Sultana, C.M., Prather, K.A., 2017. The role of jet and film drops in controlling the mixing state of submicron sea spray aerosol particle. *PNAS* July 3, 2017 114 (27), 6978–6983. <https://doi.org/10.1073/pnas.1702420114>.
- Xin, J., et al., 2016. The observation-based relationships between PM2.5 and AOD over China: the functions of PM2.5 & AOD over China. *J. Geophys. Res. Atmos.* 121, 10 701–10 716. <https://doi.org/10.1002/2015JD024655>.
- Yang, M., Bell, T.G., Hopkins, F.E., Smyth, T.J., 2016. Attribution of atmospheric sulfur dioxide over the English Channel to dimethyl sulfide and changing ship emissions. *Atmos. Chem. Phys.* 16, 4771–4783. <https://doi.org/10.5194/acp-16-4771-2016>.
- Yang, M., Huebert, B.J., Blomquist, B.W., Howell, S.G., Shank, L.M., McNaughton, C.S., Clarke, A.D., Hawkins, L.N., Russell, L.M., Covert, D.S., Coffman, D.J., Bates, T.S., Quinn, P.K., Zorogac, N., Bandy, A.R., de Szoeko, S.P., Zuidema, P.D., Tucker, S.C., Brewer, W.A., Benedict, K.B., Collett, J.L., 2011. Atmospheric sulfur cycling in the southeastern Pacific – longitudinal distribution, vertical profile, and diel variability observed during VOCALS-REx. *Atmos. Chem. Phys.* 11, 5079–5097. <https://doi.org/10.5194/acp-11-5079-2011>.
- Yang, M., Norris, S.J., Bell, T.G., Brooks, I.M., 2019. Sea spray fluxes from the southwest coast of the United Kingdom – dependence on wind speed and wave height. *Atmos. Chem. Phys.* 19, 15271–15284. <https://doi.org/10.5194/acp-19-15271-2019>.
- Yeatman, S.G., Spokes, L.J., Jickells, T.D., 2001. Comparisons of coarse-mode aerosol nitrate and ammonium at two polluted coastal sites. *Atmos. Environ.* 35 (7), 1321–1335.
- Yoon, J., Pozzer, A., Chang, D.Y., Lelieveld, J., Kim, J., Kim, M., Lee, Y.G., Koo, J.-H., Moon, K.J., 2016. Trend estimates of AERONET-observed and model-simulated AOTs between 1993 and 2013. *Atmos. Environ.* 125, 33–47.
- Zdun, A., Rozwadowska, A., Kratzer, S., 2011. Seasonal variability in the optical properties of Baltic aerosols. *Oceanologia* 53 (1), 7–34. <https://doi.org/10.5697/oc.53-1.007>.
- Zhao, B., Jiang, J.H., Gu, Y., Diner, D., Worden, J., Liou, K.-N., Su, H., Xing, J., Garay, M., Huang, L., 2017. Decadal-scale trends in regional aerosol particle properties and their linkage to emission changes. *Environ. Res. Lett.* 12 (5).
- Zhao, B., Jiang, J.H., Diner, D.J., Su, H., Gu, Y., Liou, K.-N., Jiang, Z., Huang, L., Takano, Y., Fan, X., Omar, A.H., 2018. Intra-annual variations of regional aerosol optical depth, vertical distribution, and particle types from multiple satellite and ground-based observational datasets. *Atmos. Chem. Phys.* 18, 11247–11260. <https://doi.org/10.5194/acp-18-11247-2018>.
- Zieliński, T., 2004. Studies of aerosol physical properties in coastal areas. *Aerosol. Sci. Technol.* 38 (5), 513–524. <https://doi.org/10.1080/02786820490466738>.